

1 **Photolysis of frozen iodate salts as a source of active** 2 **iodine in the polar environment**

3

4 **Óscar Galvez¹, M. Teresa Baeza-Romero², Mikel Sanz² and Alfonso Saiz-Lopez³**

5 [1]{Departamento de Física Molecular, Instituto de Estructura de la Materia, IEM-CSIC,
6 28006 Madrid, Spain}

7 [2]{Escuela de Ingeniería Industrial, Universidad de Castilla-La Mancha, 45071, Toledo,
8 Spain}

9 [3]{Department of Atmospheric Chemistry and Climate, Institute of Physical Chemistry
10 Rocasolano, CSIC, 28006 Madrid, Spain}

11

12 Correspondence to: O. Gálvez (oscar.galvez@csic.es)

13

14 **Abstract**

15 Reactive halogens play a key role in the oxidation capacity of the polar troposphere.
16 However, sources and mechanisms, particularly those involving active iodine, are still poorly
17 understood. In this paper, the photolysis of an atmospherically relevant frozen iodate salt has
18 been experimentally studied using infrared (IR) spectroscopy. The samples were generated at
19 low temperatures in the presence of different amounts of water. The IR spectra have
20 confirmed that under near-UV/Vis radiation iodate is efficiently photolyzed. The integrated
21 IR absorption coefficient of the iodate anion on the band at 750 cm^{-1} has been measured to be
22 $A=9.5\times 10^{-17}\text{ cm molec}^{-1}$. Monitoring the decay of ammonium IR band (1430 cm^{-1}) in the
23 presence of a solar simulator, which was observed to correlate with iodate anion IR band,
24 photolysis rate of ammonium iodate salt was measured. A lower limit of the integrated
25 absorption cross section of iodate, in an ammonium frozen salt, has been estimated for the
26 first time at wavelengths relevant for tropospheric studies ($\sigma=1.1\times 10^{-20}\text{ cm}^2\text{ nm}$ from 300 to
27 900 nm). According to this, we suggest that the photolysis of iodate in frozen salt can
28 potentially provide a pathway for the release of active iodine to the polar atmosphere.

1

2 **1 Introduction**

3 Atmospheric iodine compounds are present in the marine and polar boundary layers (Saiz-
4 Lopez et al., 2012), where it plays a relevant role in catalytic ozone destruction (Saiz-Lopez et
5 al., 2007b) (Read et al., 2008) and could also be involved in new particle formation in the
6 polar environment (Allan et al., 2015;Roscoe et al., 2015). Moreover, in the polar atmosphere,
7 iodine has also been suggested as one of the possible sinks of gaseous elemental mercury
8 (Calvert and Lindberg, 2004;Saiz-Lopez et al., 2008).

9 Despite the concentration of atmospheric iodine being highly variable at different regions,
10 ground- (Frieß et al., 2001) (Saiz-Lopez et al., 2007b) (Atkinson et al., 2012) and satellite-
11 based instrumentation (Saiz-Lopez et al., 2007a;Schönhardt et al., 2008) measurements have
12 confirmed remarkably high concentrations (up to 20 pptv) of IO in coastal Antarctica.
13 Nevertheless, the sources and mechanisms of iodine emissions from ice remain poorly
14 understood (Saiz-Lopez et al., 2015)(Kim et al., 2016).

15 Apart from observations of gaseous iodine species, different studies have conducted analysis
16 of the iodine fraction in rainwater (Laniewski et al., 1999) and aerosol (Baker et al., 2000). In
17 all of them, iodine concentrations are considerably enriched over seawater, and an appreciable
18 fraction of soluble iodine species like I^- and IO_3^- is observed, although the mechanism
19 determining the I^-/IO_3^- ratio is still unclear. Thus, for example since IO_3^- has been considered
20 an inert inorganic iodine species, and therefore a sink molecule in the atmospheric iodine
21 cycle, model calculations (Pechtl et al., 2006) suggest that IO_3^- should accumulate in marine
22 aerosol. However, several field campaigns (Baker, 2004;Gilfedder et al., 2008) have revealed
23 that the iodide/iodate ratio is rather variable in aerosol, showing significant I^- concentration.

24 A recent study has suggested that IO_3^- anions show a substantial reactivity in frozen solutions
25 under near-UV/Visible light irradiation (Spolaor et al., 2013). During the irradiation of IO_3^-
26 solutions reactive gaseous iodine species were produced and converted to iodine oxide
27 particles (IOP) for detection. Inspired by these results, we have further studied the photo-
28 stability of iodate frozen salts to assess its potential role in iodine emissions to the polar
29 atmosphere. In this work, we have determined for the first time the integrated absorption cross
30 section of frozen ammonium iodate solutions at wavelengths relevant for the troposphere.
31 Using this value (which should be taken as a lower limit that need to be confirmed in future
32 works), and the recorded UV-Vis spectra for the liquid solution, we have also simulated the

1 differential absorption cross section from 300 to 900 nm. This information has been
2 incorporated into an atmospheric model of the Antarctic boundary layer to assess the potential
3 of iodate photolysis to release reactive iodine in coastal Antarctica during springtime.

4 5 **2 Experimental methods**

6 For the study of the photolysis of iodate salts, we have chosen aqueous solutions of NH_4IO_3 .
7 The choice of this species was based on several reasons:

8 (i) It was not possible to monitor iodate signal in the presence of high concentration of water
9 since the infrared iodate band overlaps with water absorptions. The fact that the chosen salt
10 has a cation like NH_4^+ that presents a band with no interference (and that it is consumed in a
11 1:1 ratio with iodate) allowed us to measure the photolysis of iodate indirectly as described
12 below.

13 (ii) The integrated IR absorption coefficient of iodate band was unknown, and in
14 consequence, it was not possible to quantify the amount of iodate in the samples. One of the
15 possibilities to solve this problem is to use an iodate salt for which the integrated absorption
16 coefficient of the IR band of the counter-ion was known, like ammonium iodate. More details
17 of these calculations are given in the next section.

18 (iii) Moreover, ammonium iodate is expected to be one of the abundant iodate salts in the
19 atmosphere, since ammonium concentrations are high in some environments, and it could be
20 deposited into the ice as large fluxes of iodinated compounds have been observed during
21 glacial period (Spolaor et al., 2013), and the presence of ammonium ions in ice samples is
22 also expected. Moreover, ammonium and iodinated compounds have been detected at the
23 same time in melting Arctic sea ice, implying that this salt could be atmospherically relevant
24 (Assmy et al., 2013).

25 However, other salts like NaIO_3 or KIO_3 would be representative of polar environments also,
26 and further experiments using these compounds should be addressed in the future.

27 Solid samples containing iodate anions were produced through the sudden freezing of droplets
28 of aqueous solutions of NH_4IO_3 on a cold Si substrate located inside a vacuum chamber. A
29 detailed description of the experimental setup can be found elsewhere (Maté et al.,
30 2009;Gálvez et al., 2010), and only a brief description of the most relevant aspects for the
31 present experiments is given here. The solid substrate is mounted in a Cu block in contact

1 with a liquid nitrogen Dewar. The substrate temperature can be controlled with 1 K accuracy
2 between 90 K and 300 K. The vacuum chamber, which is coupled to a Vertex70 Bruker FTIR
3 spectrometer through a purged pathway, is evacuated with a turbomolecular pump to a
4 background pressure of $\sim 10^{-8}$ mbar. Transmission spectra of the samples were recorded, with
5 2 cm^{-1} resolution, using an MCT (Mercury Cadmium Telluride) detector refrigerated with
6 liquid nitrogen. Liquid solution droplets from a room temperature pulsed valve (General
7 Valve, series 9), usually employed for the generation of free jets and molecular beams (Abad
8 et al., 1995), were made to impinge on the cold Si substrate placed at $\sim 15\text{-}20$ mm. When a
9 desired amount of sample is on the substrate, this can be rotated to record the IR spectra, or to
10 be processed by simulated Solar light. A scheme of the experimental setup is shown in Fig. 1.
11 Solar irradiance was simulated by a 1000 W LOT® Xenon Arc lamp that radiate between
12 around 250 nm to $2.5\ \mu\text{m}$, although an important fraction of the output is given below 900 nm
13 according to the supplier of this lamp, where a fairly constant spectral irradiance is obtained
14 between 300 to 900 nm. Power light received on the substrate is measured by a portable meter
15 Thermal Detector, model 407A by Spectra-Physics, which operates in a wavelength range
16 from 250 nm to $11\ \mu\text{m}$ without significant sensitivity variations (less than 3 %).

17 UV-Vis spectra of studied salts were obtained in water solution at different concentrations
18 using an UV-Visible Uvikon spectrophotometer 930 from Kontron Instruments equipped with
19 quartz cuvettes of 10 mm size. The spectra resolution was fixed at 0.5 nm, from 190 to 500
20 nm.

21 In all experiments, pulsed valve was filled by a solution 0.1 M of ammonium iodate (Across
22 Organics, for analysis). A slight He overpressure behind the liquid solution filling the valve
23 improved the performance. This generation procedure does not lead to a uniform film, and the
24 thickness of the ice samples, which typically range from 0.1 to $1\ \mu\text{m}$ approximately (Mate et
25 al., 2012), can vary among different experiments. Solid samples generated by this technique
26 contain compact ices structures in a hyperquenched glassy water morphology (Mayer, 1985)
27 in which the water molecules retain their amorphous liquid structure, and where ions are
28 solvated by water molecules instead of being segregated in the ice (Mate et al., 2012). When
29 the temperature of substrate is below water sublimation (around 170 K), the concentration of
30 ammonium iodate salt in the ices samples is very low (comparable to the liquid solution), and
31 infrared spectra of these ice mixtures are dominated by water absorptions. In these cases,
32 water bands hide the IR features of the salt, and prevent monitoring its evolution during

1 irradiation. For this reason, most of the samples are slowly warmed above water sublimation
2 to achieve a lower water concentration to avoid that problem, or just to study dry samples
3 (although an amount of water is always present). Nevertheless, some samples were also
4 reserved in their original diluted salt proportion to explore this possible variable. We refer to
5 the samples that have suffered this process as *hyperquenched (HQ) samples*. In other
6 experiments, samples are dry, and then a controlled water vapour flux is added to be adsorbed
7 on the salt, which was kept at low temperatures (100 or 140 K) to condense water. With this
8 procedure, solid samples present a different morphology since water molecules are deposited
9 uniformly on the salt surface resulting in a more porous structure. When the condensation of
10 water occurs at 100 K, a homogeneous film of low-density amorphous water ice is deposited
11 on top of the salt. If the temperature of deposition is 140 K, the ice film has crystal cubic ice
12 structure (Mate et al., 2012). In both cases, we refer to these samples as *Vapor deposited*
13 *(Vap) samples*.

14 Initially, and it has been mentioned above, deposition at low temperature (< 120 K) leads to
15 amorphous ices samples, which show high specific surface areas (SSA) (Mate et al., 2012),
16 around 100 times higher, or even more, than typical atmospheric ice samples. However, when
17 temperature is increased amorphous samples are irreversibly transformed to crystal ice,
18 leading to a reduction of the SSA by a factor of 100 or even higher (Ocampo and Klinger,
19 1982), which are common values of freshly atmospheric ice samples.

20 Due to the requirements of the experimental setup, the ratio of $\text{NH}_4\text{IO}_3:\text{H}_2\text{O}$ in the samples is
21 considerable much higher than for environmental ices, however, some more diluted samples
22 has been studied to see the effect of this variable in the photolysis process, although always
23 our samples were much more concentrated than in natural polar conditions.

24 To summarize the procedure to generate the samples, they were firstly generated by HQ
25 deposition at 100, 140, 160, 200, 260 or 298 K. After deposition at those temperatures, three
26 different processes could be carried out: (i) the samples at the deposition temperature were
27 just irradiated, (ii) samples were firstly annealing to eliminate part of the water, then cold
28 down to a certain temperature and then irradiated, (iii) or samples were annealing until to be
29 completely dry, then cold down to a selected temperature at which a certain amount of water
30 from vapor phase was deposited, and finally irradiated.

1 **2.1 Determination of the concentration of species in the samples**

2 Column densities of water, NH_4^+ and IO_3^- ions in the ice mixtures were calculated via the
3 Lambert–Beer equation, using the integrated values of the infrared absorption bands, and the
4 corresponding integrated absorption coefficients, A . The bands chosen for this purpose were
5 the ν_2 and $\nu_2+\nu_R$ bands of water around 1650 and 2220 cm^{-1} , respectively, the ν_4 band of
6 NH_4^+ around 1430 cm^{-1} , and the ν_3 band of IO_3^- at approx. 740 cm^{-1} . For water band intensity,
7 we have used the values reported by Mastrapa *et al.* (Mastrapa *et al.*, 2009) for an amorphous
8 or crystalline phase at 100 K. For *HQ* samples the values of amorphous ice are used:
9 $A(\text{H}_2\text{O})_{\text{amorphous}} = 1.6 \times 10^{-17}$ and 9.8×10^{-18} cm molec^{-1} , while for *Vap* samples the integrated
10 absorption coefficients of cubic ice are more representative: $A(\text{H}_2\text{O})_{\text{cubic}} = 1.8 \times 10^{-17}$ and 1.1
11 $\times 10^{-17}$ cm molec^{-1} , for 1650 and 2220 cm^{-1} bands, respectively. In the case of NH_4^+ , different
12 values of the absorption coefficient have been reported in the literature, ranging from 2.5 to
13 4.4×10^{-17} cm molec^{-1} (Maté *et al.*, 2009) (Schutte and Khanna, 2003). Due to these
14 discrepancies, we have selected a suitable value of 4.0×10^{-17} cm molec^{-1} , close to that given
15 by Schutte & Khanna (Schutte and Khanna, 2003) for solid samples, which are more
16 representative of our case. For iodate, we are not aware of previous data of A values in the IR
17 region. In this case, we have estimated this value for pure ammonium iodate samples, based
18 on that previously given for NH_4^+ , obtaining a mean integrated absorption coefficients $A(\text{IO}_3^-)$
19 $= 9.5 \times 10^{-17}$ cm molec^{-1} for the band centred at 750 cm^{-1} .

20 **2.2 Calculation of spectral irradiance received by the samples**

21 We assumed that the observed photolysis of ammonium iodate samples should be mainly due
22 to the highest frequency photons emitted by the Solar lamp. The reason is that IO_3^- in aqueous
23 media absorbs light only in the UV range (Awtrey and Connick, 1951), at wavelengths below
24 270 nm, which is also in agreement with our near UV-Vis spectra of iodate salts (see Fig. 2).
25 In consequence, the UV-Vis spectrum of the glass window, through which light penetrates
26 before reaching the sample (see Fig. 1), was recorded to demarcate the transparent interval of
27 frequencies, especially the UV cutoff, see Fig. 2. Taking into account this spectrum, and in
28 combination with that provided by the lamp manufacturer for the lamp spectra and spectral
29 irradiance at 0.5 m, we estimated that only 42% of the total lamp power is emitted in the
30 wavelength interval from 300 to 900 nm. Consequently, since our Thermopile covers the
31 whole range of frequencies without significant variations, only a 42 % of the measured power

1 is due to the impinged photons of 300 to 900 nm. The average reading in the Thermopile
2 along the experiments was around 1.5 W cm^{-2} , which was regularly monitored during the
3 experiments. Thus, according to the above estimation, the substrate was irradiated with an
4 average light power of 0.66 W cm^{-2} , in the wavelength range of 300 to 900 nm. In order to
5 illustrate whether this irradiance power is characteristic of environmental conditions, we
6 estimated that around $2.8 \times 10^{15} \text{ photons cm}^{-2} \text{ s}^{-1}$ are impinging the substrate at 500 nm, which
7 result in around 8 times higher irradiance than the measured mean Solar irradiance on Earth
8 surface at mid-latitudes, ca. $3.5 \times 10^{14} \text{ photons cm}^{-2} \text{ s}^{-1}$. Nevertheless, we take into account
9 that, due to our experimental procedure, samples are not homogeneously distributed on the
10 substrate, and consequently the photon flux impacting on the samples was, to a certain degree,
11 lower. This consideration is further explored in the following section.

12

13 **3 Results and Discussions**

14 **3.1 Laboratory experiments**

15 Fig. 3 shows IR spectra of different samples of solid ammonium iodate salt at 200 and 100 K
16 including those of 3.6 and 2.1 $\text{H}_2\text{O}/\text{NH}_4\text{IO}_3$ ice mixtures deposited at 100 K obtained by the
17 hyperquenching (*HQ*) technique or via vapor deposited (*Vap*) H_2O , respectively. Table 1
18 displays the positions of bands of the IR spectra of NH_4IO_3 shown in Fig. 3. Sharper and more
19 defined bands appear in spectra at 100 K, showing also a slight displacement, which are
20 typical effects when temperature is decreased (Gálvez et al., 2009). When water is present,
21 IO_3^- bands undergo a small blue-shift, which can be related to the overlap with the ν_{R} libration
22 water mode at ca. 800 cm^{-1} . Moreover, some differences in the water bands become visible on
23 the spectra of the mixtures, arising from the solid structure of water ice. In the *HQ* sample
24 show in the figure, the initial deposited ice mixture at 100 K is slightly warmed to 200 K to
25 dry the sample and to achieve the water/salt composition desired and then cold down to 100 K
26 for recording the spectrum. Therefore, in this process, initial amorphous water matrix is
27 crystallized during annealing, showing an IR spectrum typical of a cubic phase. In the case of
28 *Vap* samples, initial deposits at 100 K are completely dried at high temperature, and, after
29 decreasing to 100 K, water is added at this temperature to achieve the water/salt composition
30 required. Therefore, in this case, water ice shows a low-density amorphous structure, which
31 corresponds to deposition at 100 K, showing broader bands in the IR spectrum.

1 After generation, samples were irradiated during 3 to 5 hours by a 1000 W Xenon Arc lamp.
2 This process has been carried out for all samples generated by means of the different
3 procedures mentioned in the experimental section. In all samples NH_4^+ and IO_3^- IR bands
4 diminish during irradiation process, which is especially evident when 1430 and 745 cm^{-1}
5 bands are monitored. The photo-reduction of iodate in solid or ice samples has recently been
6 suggested by Spolaor *et al.* (Spolaor et al., 2013). To illustrate this effect, Figure 4 shows the
7 relation between the integrated infrared intensity on these bands for some pure samples
8 irradiate at different temperatures, revealing the linear correlation existing between these
9 values during the irradiation process (typical R^2 value higher than 0.99). Note that this
10 correlation is more difficult to examine in the case of H_2O /salt mixtures, since both i) the
11 overlap of water and IO_3^- bands, ii) and the different changes that integrated absorption
12 coefficients of NH_4^+ and IO_3^- infrared bands could undergo in the presence of water, due to
13 the intermolecular hydrogen bond formed in the hydration process. Nevertheless, and taking
14 into account these considerations, the linear correlation (higher than 0.9) between both
15 integral values can be observed in these cases, too, although it is not shown here.

16 Is important to highlight that not any evolution of the IR spectra of the samples was observed
17 in dark conditions (this fact was checked many times along the experimental campaign).

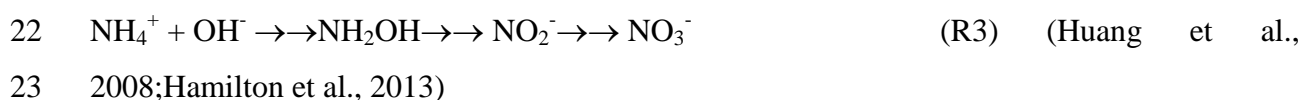
18 Typical UV-Vis spectra of common ammonium salts (i.e. NH_4Cl) do not display significant
19 absorption bands in the near- UV and visible regions (see Fig. 2), and, to the best of our
20 knowledge, no literature exists on the photolysis of this species. Based on this, the photolysis
21 of ammonium ions is not expected to occur in this spectral range. Consequently, reduction of
22 the IR ammonium bands should be caused by a fast reaction with “reacting” species produced
23 by photolysis of frozen iodate during the irradiation process: HOI , IO and I_2 (Spolaor et al.,
24 2013), or OIO (Klaning et al., 1981), or other reacting species (e.g.: oxygen atoms or anions,
25 see above). We observed that iodine reacts with ammonia in aqueous solution (McAlpine,
26 1952), and consequently, we expected that any of these iodinated compounds obtained, which
27 could be even more reactive than I_2 , could react very fast with the present NH_4^+ .

28 In addition to those at the 1430 and 740 cm^{-1} bands, other changes are evident in the IR
29 spectra, revealing that not only ammonium and iodate ions are consumed, but also new
30 products are formed. These changes are more evident in the low temperature experiments,
31 around 100 K, since volatile products formed during the photolysis can also be retained on the
32 substrate. Figure 5 shows an example of a pure solid NH_4IO_3 salt deposited at 100 K and

1 irradiated at that temperature. Dotted lines indicate bands that undergo clear changes during
2 the photolysis.

3 Stretching of the NH_4^+ bands around 3000 cm^{-1} diminishes with irradiation, although an
4 increase of water band intensities, more evident in the peak around 3360 cm^{-1} , also occurs,
5 probably due to the residual water background always present in the chamber (note that this
6 effect only occurs at temperatures below 150 K). Two new peaks emerge during photolysis,
7 around 2227 and 1300 cm^{-1} . The first one is only visible at 100 K but the low frequency peak
8 can also be observed at higher temperatures. The bands around 2227 cm^{-1} could belong to
9 infrared absorptions of C-O stretching modes. Slight carbon contamination mainly by CO_2
10 molecules are usually found in this type of experiments (Mate et al., 2014). Another
11 possibility could be the formation of N_2O molecules which bear infrared signal around 2200
12 cm^{-1} . The band around 1300 cm^{-1} can also be caused by N-O stretching vibration, which could
13 be formed by reaction of O^* species with ammonium. Nevertheless, all these assignments
14 should be considered as speculative.

15 According to the peaks observed as products in the IR spectra, the behaviour of reactant's IR
16 peaks, and previous work on laser flash photolysis of iodate aqueous solution (Klaning et al.,
17 1981) and photolysis of ice samples (Spolaor et al., 2013), we tentatively proposed the
18 following possible mechanism for the photolysis of ammonium iodate ice, although further
19 experiments are required to confirm it:



25 where R2 and R3 need to be very fast reactions since the photolysis rates of IO_3^- and NH_4^+
26 were equivalent. OIO, IO, I and I_2 or even HOI (by reaction of I or IO with OH/ HO_2) could be
27 the active iodine products that are released to the atmosphere.

28 According to this mechanism, OIO is the initial iodine species formed. The IR band for this
29 compound is about 800 cm^{-1} (Maier and Bothur, 1997), and consequently, it cannot be
30 monitored due to its overlap with the IO_3^- band. Nevertheless, as was mentioned above, more

1 studies should be carried out to further understand and corroborate this tentative mechanism
2 proposed.

3 However, independently of the mechanism of the photolytic process, the photolytic rate
4 constant, J value, for the iodate ion can be calculated according to equation E1:

$$5 \quad -\frac{d[IO_3^-]}{dt} = J[IO_3^-] \quad (E1)$$

6 The concentration of iodate ion can be monitored by integration of the infrared band intensity
7 at ca. 740 cm^{-1} , that, as shown in Fig. 4, is equivalent to monitor the NH_4^+ band at 1430 cm^{-1} :

$$8 \quad -\frac{d[IO_3^-]}{dt} = J[IO_3^-] \quad \ll==\gg \quad -\frac{d[NH_4^+]}{dt} = J[NH_4^+] \quad (E2)$$

9 Integrating E2 and considering that concentration is proportional to IR band intensity:

$$10 \quad \ln(I_t) = \ln(I_0) - Jt \quad (E3)$$

11 where I_t and I_0 are the intensity of the band of NH_4^+ (or IO_3^-) at time t and zero, respectively.

12 According to E3, a representation of the natural logarithm of the integrated band intensities of
13 NH_4^+ or IO_3^- signals versus time of photolysis will give us the J value, as the slope of the line
14 of the best linear fit. This calculation has been done for all deposited samples at different
15 temperatures and water concentrations (see Figure 6 as an example for some of the samples).
16 Integration limits of the bands differ among the different samples, due to baseline of the
17 spectra are rather sensitive to the generation process and morphologies of the ices mixtures.
18 For this reason, the integration limits of the bands were adjusted for each sample studied in
19 order to minimize the errors during this process. The calculated mean value for all
20 experiments carried out (at an average light power of 0.66 W cm^{-2} , see above) is $J = (4 \pm 2) \times$
21 10^{-5} s^{-1} . Significant differences in the J values have not been observed among the samples
22 prepared at different conditions, i.e. *Vap o HQ* deposition of water, different temperatures of
23 generation and irradiation (from 100 to 298 K) or different amount of water in the mixtures,
24 although in this last case, for more diluted samples the resulting J values are usually higher in
25 absolute terms (the average J value considering only diluted samples is around 10 % higher).
26 This effect could be due to a larger surface/bulk ratio in diluted samples, although in any case,
27 it is always within the experimental uncertainties. The fact that not significant variations on
28 the calculated J values were obtaining in the experiments point to the photo-reduction process
29 do not notably depends on the morphology of the ices, at least in the range of samples studied.

1 If the photolysis rate and the radiative flux are known, the integrated cross section of the
2 iodate ion can be estimated according to E4:

$$3 \quad J = \int_{\lambda_1}^{\lambda_2} F(\lambda)\sigma(\lambda)\phi(\lambda)d\lambda \quad (\text{E4})$$

4 where $F(\lambda)$ is the radiative flux, $\sigma(\lambda)$ is the absorption cross section and $\phi(\lambda)$ is the quantum
5 yield of the photolysis reaction. The radiative flux employed in the experiment has been
6 calculated previously (see experimental section). If we assume a constant quantum yield of
7 unity in the interval, the integrated absorption cross section from 300 to 900 nm yields a value
8 of $(1.1 \pm 0.6) \times 10^{-20} \text{ cm}^2 \text{ nm}$. For comparison purposes, the integrated cross section of O_3 in the
9 spectral interval 410–690 nm (Chappuis band) is around $6.6 \times 10^{-20} \text{ cm}^2 \text{ nm}$ (Bogumil et al.,
10 2001).

11 The assumption of a constant quantum yield of unity in the interval should be regarded with
12 caution. It is known that this value depends not only on the wavelength value but the dilution
13 and conditions of the samples, too (as for example on their aggregation phase) (Rahn et al.,
14 2003). However, there is no information about this value for any frozen iodate frozen salt, and
15 in consequence the integrated cross section determined in this study assumes that the quantum
16 yield of the photolysis process.

17 In order to estimate the near visible absorption of iodate salts, UV-Vis spectra were recorded
18 for water solution of NH_4IO_3 , NH_4Cl and KIO_3 salts (see Fig. 2). In all cases, nearly null
19 absorptions were recorded above 300 nm. These results are in agreement with that of
20 Saunders *et al.*, (Saunders et al., 2012) and Awtrey and Connick, (Awtrey and Connick, 1951),
21 who also found nearly null absorption above 300 nm for NaIO_3 salt solutions. According to
22 these results, the photo-reactivity of the iodate salts should be related to the low-temperature
23 effect, and the fact that iodate solutions or salts are frozen, in agreement with the results from
24 Spolaor *et al.* (Spolaor et al., 2013). It is well known that different photochemical reactions are
25 greatly accelerated in frozen solution due, for example, by the concentration of solutes in
26 porous or channel formed in the water ice network (see e.g. Grannas *et al.* (Grannas et al.,
27 2007) and references therein).

28 To provide an estimation of the variation of the absorption cross section in this spectral
29 interval, we can use as a reference the spectral shape of the NH_4IO_3 solutions showed in Fig.
30 2. According to this, it seems reasonable to approximate the spectral shape to a decay tail of a
31 Gaussian function (although no significant differences would be obtained if a Lorentzian

1 function would be used) peaking in 205 nm (according to the spectrum of 9.6×10^{-4} M
2 NH_4IO_3 shown in Figure 2), which is presented in Fig. 7. The total area of the Gaussian
3 function simulation (from 300 to 900 nm) has been fixed to the previous calculated value for
4 the integrated absorption cross section, and the width of the Gaussian function has arbitrarily
5 selected to force that approx. 95 % of the value of the integrated cross section would be in the
6 range from 300 to 500 nm. In this calculation, a σ of $1.35 \times 10^{-22} \text{ cm}^2$ is obtained at 350 nm, a
7 value, for example, relatively close to that recorded for O_3 at this frequency, approx. 4×10^{-22}
8 cm^2 (Burrows et al., 1999), but quite far lower than the one for NO_3 at 662 nm that is $1.90 \times$
9 10^{-17} cm^2 at 298 K (Ravishankara and Mauldin, 1986).

10 However, due to the above mentioned limitations in our experimental set-up the integrated
11 absorption cross-section of iodate should be regarded as a lower limit. The reason is mainly
12 the limitations associated with distributing the samples homogeneously during deposition,
13 which could generate areas free of samples on the substrate. For these cases, the irradiance
14 received by the samples could be lower than calculated (which assume a homogeneous
15 distribution of the sample), leading finally to a higher calculated absorption cross section
16 value than the one obtained in this work. Based on the dispersion of our results, we have
17 estimated that this effect could account for an increase on this value by up to a factor of two.
18 In addition, diluted samples showed an increase of the J values of around 10 %, which,
19 although in within experimental limitations, also would cause a higher absorption cross
20 section value. In conclusion, both effects could account for a cross section value up to an
21 order of magnitude higher than that reported here, so we emphasize that it should be
22 considered as a lower limit. Nevertheless, further experiments should be done to confirm the
23 integrated absorption cross section value.

24

25 **3.2 Model simulations**

26 In spite of the experimental limitations mentioned above, we have incorporated the
27 experimentally-derived absorption cross section value into an atmospheric model in order to
28 assess the implications that this process could have in polar atmospheric chemistry.

29 Although high levels of reactive iodine have been measured in coastal Antarctica, the
30 emission mechanism over ice still remains unclear. We use an atmospheric model (for details
31 see Saiz-Lopez et al.(Saiz-Lopez et al., 2008)) of the Antarctic boundary layer to assess the

1 potential of iodate photolysis to release reactive iodine to the polar atmosphere. The model is
2 initialized with typical concentrations of atmospheric constituents in coastal Antarctica (Jones
3 et al., 2008) for October. We constrain the ice surface in the model with an average iodate
4 concentration at the ice surface of 19 nM, as recently measured over the Weddell Sea
5 (Atkinson et al., 2012). The model incorporates a 2-stream radiation code to compute the
6 actinic flux at the surface for springtime Antarctic irradiation conditions (Saiz-Lopez et al.,
7 2008), and the mean iodate integrated absorption cross section estimated in this work, which
8 again recall that it is a lower limit. We assume that there is an iodine atom unity conversion of
9 iodate into reactive gas phase following iodate photolysis. The model results indicate that the
10 photoreduction of iodate in ice, and subsequent equilibration of the reactive iodine species,
11 yields atmospheric IO levels around 1-1.5 pptv. These levels of IO are lower than the highest
12 values measured in the biologically-active Weddell Sea region. However, lower IO
13 concentrations have also been reported in other coastal regions away from the Weddell Sea
14 (Schönhardt et al., 2008). We would like to highlight that the IO concentration given by the
15 model is proportional to the cross section values used for iodate, so much larger IO levels
16 could be obtained. The photolysis of iodate could provide a source of iodine that accounts for
17 some of the comparatively low levels observed, and, to a lesser extent, also contribute to the
18 iodine emissions over the Weddell Sea zone. Note that the model does not consider the
19 potential loss at the ice surface of the iodine photofragments resulting from the iodate
20 photolysis. The model results suggest, within the uncertainties highlighted above, that the
21 photolysis of iodate on the surface of ice can potentially constitute an abiotic pathway for the
22 release of active iodine to the polar atmosphere. Further laboratory and field work is needed
23 to better assess the environmental implications of iodate photolysis in the ice.

24

25 **4 Conclusions**

26 We have explored the photolysis of ammonium iodate salt in frozen solutions. The samples
27 were generated by different deposition methods, and at different temperatures and water
28 concentrations, in order to obtain samples of different morphologies. The samples were
29 processed by simulated Solar light with an average light power of 0.66 W cm^{-2} , in the
30 wavelength range of 300 to 900 nm. In all cases, the evolution of the IR spectra confirms the
31 photolysis of iodate salt for all samples in a similar way. The photolysis rates obtained are
32 similar for all the samples generated, within our experimental uncertainties. The bands of

1 NH_4^+ and IO_3^- decrease during irradiation and new small bands appear, too. A tentative
2 mechanism of the photolysis process is presented, in which OIO is formed as a first step of
3 the photolysis of iodate. Both OIO and other reactive iodine species, which could be formed
4 in subsequent reactions (IO , I_2 , HOI , etc.), could be released to the gas phase. As result of
5 these experiments, the integrated absorption cross section of iodate in an ammonium frozen
6 salt has been estimated for the first time at wavelengths relevant for tropospheric studies ($\sigma =$
7 $(1.1 \pm 0.6) \times 10^{-20} \text{ cm}^2 \text{ nm}$ from 300 to 900 nm). However, due to the experimental
8 limitations, this value has to be considered mainly as a lower limit, and further experiments
9 are needed to confirm it. A simulated absorption cross section in this interval region has also
10 been proposed, which has been included in an atmospheric model of the Antarctic boundary
11 layer to assess its potential environmental relevance. The model predicts that the photolysis of
12 iodate in ice could yield atmospheric IO levels around 1-1.5 pptv, which could be higher if we
13 consider a larger absorption cross sections value for the photolysis of iodate. According to
14 this, we suggest that the photolysis of iodate on the surface of ice can potentially constitute a
15 pathway for the release of active iodine to the polar atmosphere.

16

17 **Acknowledgements**

18 O. G. acknowledges financial support from Ministerio de Ciencia e Innovación, “Ramón y
19 Cajal” program and financial support from Ministerio de Economía y Competitividad, project
20 “CGL2013-48415-C2-1-R”. M.T.B-R and M.S. acknowledge financial support from
21 Ministerio de Economía y Competitividad, project “CGL2013-48415-C2-2”. O. G., M.T.B-R
22 and M.S. acknowledge financial support from the Spanish crowdfunding platform
23 PRECIPITA from FECYT foundation.

24

25

1 References

- 2 Abad, L., Bermejo, D., Herrero, V. J., Santos, J., and Tanarro, I.: Performance of a solenoid-
3 driven pulsed molecular-beam source, *Review of Scientific Instruments*, 66, 3826-3832,
4 doi:<http://dx.doi.org/10.1063/1.1145444>, 1995.
- 5 Allan, J. D., Williams, P. I., Najera, J., Whitehead, J. D., Flynn, M. J., Taylor, J. W., Liu, D.,
6 Darbyshire, E., Carpenter, L. J., Chance, R., Andrews, S. J., Hackenberg, S. C., and
7 McFiggans, G.: Iodine observed in new particle formation events in the Arctic atmosphere
8 during ACCACIA, *Atmos. Chem. Phys.*, 15, 5599-5609, 10.5194/acp-15-5599-2015, 2015.
- 9 Assmy, P., Ehn, J. K., Fernández-Méndez, M., Hop, H., Katlein, C., Sundfjord, A., Bluhm,
10 K., Daase, M., Engel, A., Fransson, A., Granskog, M. A., Hudson, S. R., Kristiansen, S.,
11 Nicolaus, M., Peeken, I., Renner, A. H. H., Spreen, G., Tatarek, A., and Wiktor, J.: Floating
12 Ice-Algal Aggregates below Melting Arctic Sea Ice, *PLoS ONE*, 8, e76599,
13 10.1371/journal.pone.0076599, 2013.
- 14 Atkinson, H. M., Huang, R. J., Chance, R., Roscoe, H. K., Hughes, C., Davison, B.,
15 Schönhardt, A., Mahajan, A. S., Saiz-Lopez, A., Hoffmann, T., and Liss, P. S.: Iodine
16 emissions from the sea ice of the Weddell Sea, *Atmos. Chem. Phys.*, 12, 11229-11244,
17 10.5194/acp-12-11229-2012, 2012.
- 18 Awtrey, A. D., and Connick, R. E.: The Absorption Spectra of I₂, I₃⁻, I⁻, IO₃⁻, S₄O₆⁼ and
19 S₂O₃⁼. Heat of the Reaction I₃⁻ = I₂ + I⁻, *Journal of the American Chemical Society*, 73,
20 1842-1843, 10.1021/ja01148a504, 1951.
- 21 Baker, A. R., Thompson, D., Campos, M. L. A. M., Parry, S. J., and Jickells, T. D.: Iodine
22 concentration and availability in atmospheric aerosol, *Atmospheric Environment*, 34, 4331-
23 4336, [http://dx.doi.org/10.1016/S1352-2310\(00\)00208-9](http://dx.doi.org/10.1016/S1352-2310(00)00208-9), 2000.
- 24 Baker, A. R.: Inorganic iodine speciation in tropical Atlantic aerosol, *Geophysical Research*
25 *Letters*, 31, n/a-n/a, 10.1029/2004gl020144, 2004.
- 26 Bogumil, K., Orphal, J., Burrows, J. P., and Flaud, J. M.: Vibrational progressions in the
27 visible and near-ultraviolet absorption spectrum of ozone, *Chemical Physics Letters*, 349,
28 241-248, [http://dx.doi.org/10.1016/S0009-2614\(01\)01191-5](http://dx.doi.org/10.1016/S0009-2614(01)01191-5), 2001.
- 29 Burrows, J. P., Richter, A., Dehn, A., Deters, B., Himmelmann, S., Voigt, S., and Orphal, J.:
30 Atmospheric remote-sensing reference data from GOME---2. Temperature-dependent
31 absorption cross sections of O₃ in the 231-794 nm range, *Journal of Quantitative*
32 *Spectroscopy and Radiative Transfer*, 61, 509-517, [http://dx.doi.org/10.1016/S0022-](http://dx.doi.org/10.1016/S0022-4073(98)00037-5)
33 [4073\(98\)00037-5](http://dx.doi.org/10.1016/S0022-4073(98)00037-5), 1999.
- 34 Calvert, J. G., and Lindberg, S. E.: The potential influence of iodine-containing compounds
35 on the chemistry of the troposphere in the polar spring. II. Mercury depletion, *Atmospheric*
36 *Environment*, 38, 5105-5116, <http://dx.doi.org/10.1016/j.atmosenv.2004.05.050>, 2004.
- 37 Frieß, U., Wagner, T., Pundt, I., Pfeilsticker, K., and Platt, U.: Spectroscopic measurements of
38 tropospheric iodine oxide at Neumayer Station, Antarctica, *Geophysical Research Letters*, 28,
39 1941-1944, 10.1029/2000gl012784, 2001.
- 40 Gálvez, O., Maté, B., Herrero, V. J., and Escribano, R.: Ammonium and Formate Ions in
41 Interstellar Ice Analogs, *The Astrophysical Journal*, 724, 539, 2010.
- 42 Gálvez, Ó., Maté, B., Martín-Llorente, B., Herrero, V. J., and Escribano, R.: Phases of Solid
43 Methanol, *The Journal of Physical Chemistry A*, 113, 3321-3329, 10.1021/jp810239r, 2009.

- 1 Gilfedder, B. S., Lai, S. C., Petri, M., Biester, H., and Hoffmann, T.: Iodine speciation in rain,
2 snow and aerosols, *Atmos. Chem. Phys.*, 8, 6069-6084, 10.5194/acp-8-6069-2008, 2008.
- 3 Grannas, A. M., Jones, A. E., Dibb, J., Ammann, M., Anastasio, C., Beine, H. J., Bergin, M.,
4 Bottenheim, J., Boxe, C. S., Carver, G., Chen, G., Crawford, J. H., Dominé, F., Frey, M. M.,
5 Guzmán, M. I., Heard, D. E., Helmig, D., Hoffmann, M. R., Honrath, R. E., Huey, L. G.,
6 Hutterli, M., Jacobi, H. W., Klán, P., Lefer, B., McConnell, J., Plane, J., Sander, R., Savarino,
7 J., Shepson, P. B., Simpson, W. R., Sodeau, J. R., von Glasow, R., Weller, R., Wolff, E. W.,
8 and Zhu, T.: An overview of snow photochemistry: evidence, mechanisms and impacts,
9 *Atmos. Chem. Phys.*, 7, 4329-4373, 10.5194/acp-7-4329-2007, 2007.
- 10 Hamilton, J. F., Baeza-Romero, M. T., Finessi, E., Rickard, A. R., Healy, R. M., Peppe, S.,
11 Adams, T. J., Daniels, M. J. S., Ball, S. M., Goodall, I. C. A., Monks, P. S., Borrás, E., and
12 Muñoz, A.: Online and offline mass spectrometric study of the impact of oxidation and ageing
13 on glyoxal chemistry and uptake onto ammonium sulfate aerosols, *Faraday Discussions*, 165,
14 447-472, 10.1039/c3fd00051f, 2013.
- 15 Huang, L., Li, L., Dong, W., Liu, Y., and Hou, H.: Removal of Ammonia by OH Radical in
16 Aqueous Phase, *Environmental Science & Technology*, 42, 8070-8075, 10.1021/es8008216,
17 2008.
- 18 Jones, A. E., Wolff, E. W., Salmon, R. A., Bauguitte, S. J. B., Roscoe, H. K., Anderson, P. S.,
19 Ames, D., Clemitshaw, K. C., Fleming, Z. L., Bloss, W. J., Heard, D. E., Lee, J. D., Read, K.
20 A., Hamer, P., Shallcross, D. E., Jackson, A. V., Walker, S. L., Lewis, A. C., Mills, G. P.,
21 Plane, J. M. C., Saiz-Lopez, A., Sturges, W. T., and Worton, D. R.: Chemistry of the
22 Antarctic Boundary Layer and the Interface with Snow: an overview of the CHABLIS
23 campaign, *Atmos. Chem. Phys.*, 8, 3789-3803, 10.5194/acp-8-3789-2008, 2008.
- 24 Kim, K., Yabushita, A., Okumura, M., Saiz-Lopez, A., Cuevas, C. A., Blaszczyk-Boxe, C. S.,
25 Min, D. W., Yoon, H.-I., and Choi, W.: Production of molecular iodine and triiodide in the
26 frozen solution of iodide: implication for polar atmosphere, *Environmental Science &*
27 *Technology*, 10.1021/acs.est.5b05148, 2016.
- 28 Klaning, U. K., Sehested, K., and Wolff, T.: Laser flash photolysis and pulse radiolysis of
29 iodate and periodate in aqueous solution. Properties of iodine(VI), *Journal of the Chemical*
30 *Society, Faraday Transactions 1: Physical Chemistry in Condensed Phases*, 77, 1707-1718,
31 10.1039/f19817701707, 1981.
- 32 Klaning, U. K., Larsen, E., and Sehested, K.: Oxygen Atom Exchange in Aqueous Solution
33 by $O + H_2O \rightarrow OH + OH$ and $OH + H_2O \rightarrow H_2O + OH$. A Study of Hydrogen
34 Atom Transfer, *The Journal of Physical Chemistry*, 98, 8946-8951, 10.1021/j100087a022,
35 1994.
- 36 Laniewski, K., Borén, H., and Grimvall, A.: Fractionation of halogenated organic matter
37 present in rain and snow, *Chemosphere*, 38, 393-409, [http://dx.doi.org/10.1016/S0045-](http://dx.doi.org/10.1016/S0045-6535(98)00181-7)
38 [6535\(98\)00181-7](http://dx.doi.org/10.1016/S0045-6535(98)00181-7), 1999.
- 39 Maier, G., and Bothur, A.: Matrix-Isolation of Iodine Superoxide and Iodine Dioxide,
40 *Chemische Berichte*, 130, 179-181, 10.1002/cber.19971300207, 1997.
- 41 Mastrapa, R. M., Sandford, R. M., Roush, T. L., Cruikshank, D. P., and Dalle Ore, C. M.:
42 Optical Constants of Amorphous and Crystalline H₂O-ice: 2.5-22 μm (4000-455 cm^{-1})
43 Optical Constants of H₂O-ice, *The Astrophysical Journal*, 701, 1347, 2009.

- 1 Mate, B., Rodriguez-Lazcano, Y., and Herrero, V. J.: Morphology and crystallization kinetics
2 of compact (HGW) and porous (ASW) amorphous water ice, *Physical Chemistry Chemical*
3 *Physics*, 14, 10595-10602, 10.1039/c2cp41597f, 2012.
- 4 Mate, B., Tanarro, I., Moreno, M. A., Jimenez-Redondo, M., Escribano, R., and Herrero, V.
5 J.: Stability of carbonaceous dust analogues and glycine under UV irradiation and electron
6 bombardment, *Faraday Discussions*, 168, 267-285, 10.1039/c3fd00132f, 2014.
- 7 Maté, B., Gálvez, O., Herrero, V. J., Fernández-Torre, D., Moreno, M. A., and Escribano, R.:
8 Water-Ammonium ICES and the Elusive 6.85 μm Band, *The Astrophysical Journal Letters*,
9 703, L178, 2009.
- 10 Mayer, E.: New method for vitrifying water and other liquids by rapid cooling of their
11 aerosols, *Journal of Applied Physics*, 58, 663-667, doi:<http://dx.doi.org/10.1063/1.336179>,
12 1985.
- 13 McAlpine, R. K.: The Reaction of Dilute Iodine and Ammonia Solutions, *Journal of the*
14 *American Chemical Society*, 74, 725-727, 10.1021/ja01123a041, 1952.
- 15 Ocampo, J., and Klinger, J.: Adsorption of N₂ and CO₂ on ice, *Journal of Colloid and*
16 *Interface Science*, 86, 377-383, [http://dx.doi.org/10.1016/0021-9797\(82\)90083-2](http://dx.doi.org/10.1016/0021-9797(82)90083-2), 1982.
- 17 Pechtl, S., Lovejoy, E. R., Burkholder, J. B., and von Glasow, R.: Modeling the possible role
18 of iodine oxides in atmospheric new particle formation, *Atmos. Chem. Phys.*, 6, 505-523,
19 10.5194/acp-6-505-2006, 2006.
- 20 Rahn, R. O., Stefan, M. I., Bolton, J. R., Goren, E., Shaw, P.-S., and Lykke, K. R.: Quantum
21 Yield of the Iodide-Iodate Chemical Actinometer: Dependence on Wavelength and
22 Concentration¶, *Photochemistry and Photobiology*, 78, 146-152, 10.1562/0031-
23 8655(2003)0780146qyotic2.0.co2, 2003.
- 24 Ravishankara, A. R., and Mauldin, R. L.: Temperature dependence of the NO₃ cross section
25 in the 662-nm region, *Journal of Geophysical Research: Atmospheres*, 91, 8709-8712,
26 10.1029/JD091iD08p08709, 1986.
- 27 Read, K. A., Mahajan, A. S., Carpenter, L. J., Evans, M. J., Faria, B. V. E., Heard, D. E.,
28 Hopkins, J. R., Lee, J. D., Moller, S. J., Lewis, A. C., Mendes, L., McQuaid, J. B., Oetjen, H.,
29 Saiz-Lopez, A., Pilling, M. J., and Plane, J. M. C.: Extensive halogen-mediated ozone
30 destruction over the tropical Atlantic Ocean, *Nature*, 453, 1232-1235,
31 http://www.nature.com/nature/journal/v453/n7199/supinfo/nature07035_S1.html, 2008.
- 32 Roscoe, H. K., Jones, A. E., Brough, N., Weller, R., Saiz-Lopez, A., Mahajan, A. S.,
33 Schoenhardt, A., Burrows, J. P., and Fleming, Z. L.: Particles and iodine compounds in
34 coastal Antarctica, *Journal of Geophysical Research: Atmospheres*, 120, 7144-7156,
35 10.1002/2015jd023301, 2015.
- 36 Saiz-Lopez, A., Chance, K., Liu, X., Kurosu, T. P., and Sander, S. P.: First observations of
37 iodine oxide from space, *Geophysical Research Letters*, 34, n/a-n/a, 10.1029/2007gl030111,
38 2007a.
- 39 Saiz-Lopez, A., Mahajan, A. S., Salmon, R. A., Bauguitte, S. J.-B., Jones, A. E., Roscoe, H.
40 K., and Plane, J. M. C.: Boundary Layer Halogens in Coastal Antarctica, *Science*, 317, 348-
41 351, 10.1126/science.1141408, 2007b.
- 42 Saiz-Lopez, A., Plane, J. M. C., Mahajan, A. S., Anderson, P. S., Bauguitte, S. J. B., Jones, A.
43 E., Roscoe, H. K., Salmon, R. A., Bloss, W. J., Lee, J. D., and Heard, D. E.: On the vertical

1 distribution of boundary layer halogens over coastal Antarctica: implications for O₃, HO_x,
2 NO_x and the Hg lifetime, *Atmos. Chem. Phys.*, 8, 887-900, 10.5194/acp-8-887-2008, 2008.

3 Saiz-Lopez, A., Plane, J. M. C., Baker, A. R., Carpenter, L. J., von Glasow, R., Gómez
4 Martín, J. C., McFiggans, G., and Saunders, R. W.: Atmospheric Chemistry of Iodine,
5 *Chemical Reviews*, 112, 1773-1804, 10.1021/cr200029u, 2012.

6 Saiz-Lopez, A., Blaszczyk-Boxe, C. S., and Carpenter, L. J.: A mechanism for biologically-
7 induced iodine emissions from sea-ice, *Atmos. Chem. Phys.*, 15, 9731-9746, 10.5194/acp-15-
8 9731-2015, 2015.

9 Saunders, R. W., Kumar, R., MacDonald, S. M., and Plane, J. M. C.: Insights into the
10 Photochemical Transformation of Iodine in Aqueous Systems: Humic Acid Photosensitized
11 Reduction of Iodate, *Environmental Science & Technology*, 46, 11854-11861,
12 10.1021/es3030935, 2012.

13 Schönhardt, A., Richter, A., Wittrock, F., Kirk, H., Oetjen, H., Roscoe, H. K., and Burrows, J.
14 P.: Observations of iodine monoxide columns from satellite, *Atmos. Chem. Phys.*, 8, 637-653,
15 10.5194/acp-8-637-2008, 2008.

16 Schutte, W. A., and Khanna, R. K.: Origin of the 6.85 micron band near young stellar objects:
17 The ammonium ion (NH₄⁺) revisited, *A&A*, 398, 1049-1062, 2003.

18 Spolaor, A., Vallelonga, P., Plane, J. M. C., Kehrwald, N., Gabrieli, J., Varin, C., Turetta, C.,
19 Cozzi, G., Kumar, R., Boutron, C., and Barbante, C.: Halogen species record Antarctic sea ice
20 extent over glacial–interglacial periods, *Atmos. Chem. Phys.*, 13, 6623-6635, 10.5194/acp-13-
21 6623-2013, 2013.

22
23
24
25

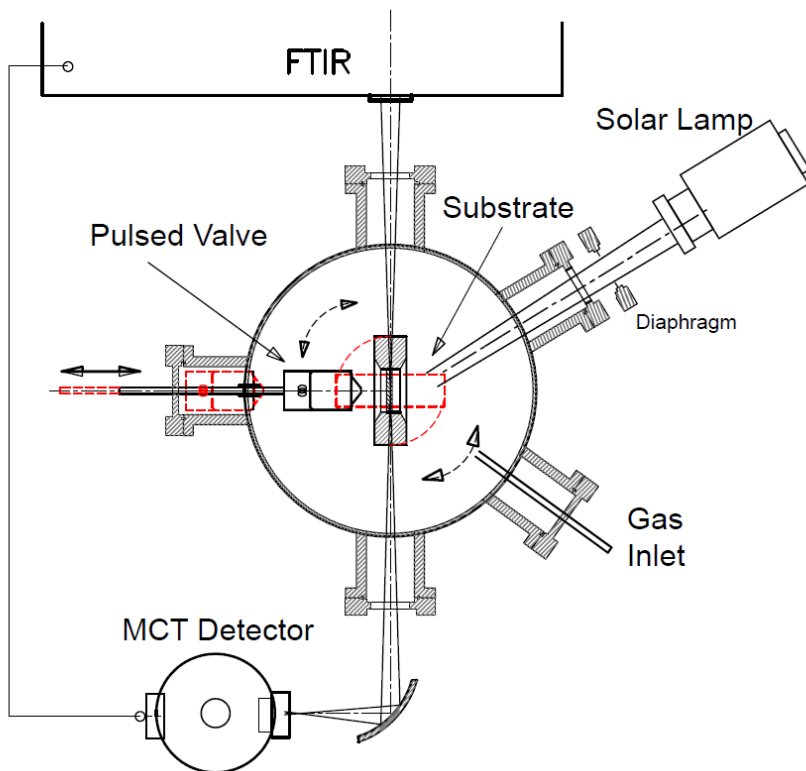
1 **Table 1.** Positions (in cm^{-1}) and assignment of the mid-IR spectra bands of the NH_4IO_3 salt
 2 shown in Fig. 2.

Experiment	$\nu_1, \nu_3 (\text{IO}_3^-)$	$\nu_4 (\text{NH}_4^+)$	$2\nu_1, \nu_3 (\text{IO}_3^-)?$	$2\nu_4, \nu_2 + \nu_4, \nu_3 (\text{NH}_4^+)$
NH_4IO_3 200 K	742, 792 ^{sh}	1428, 1451 ^{sh}	1683	2839, 3020, 3165
NH_4IO_3 100 K	738, 772 ^{sh} , 792 ^{sh}	1432, 1456 ^{sh}	1683	2839, 3020, 3154
3.6 $\text{H}_2\text{O}/\text{NH}_4\text{IO}_3$ 100 K HQ	745, 769 ^{sh} , 794 ^{sh}	1432, 1456 ^{sh}	1683	2839, 3020, 3154 ^{sh}
2.1 $\text{H}_2\text{O}/\text{NH}_4\text{IO}_3$ 100 K Vap	749, 792 ^{sh}	1432, 1456 ^{sh}	1683	2839, 3020, 3154 ^{sh}

3

4

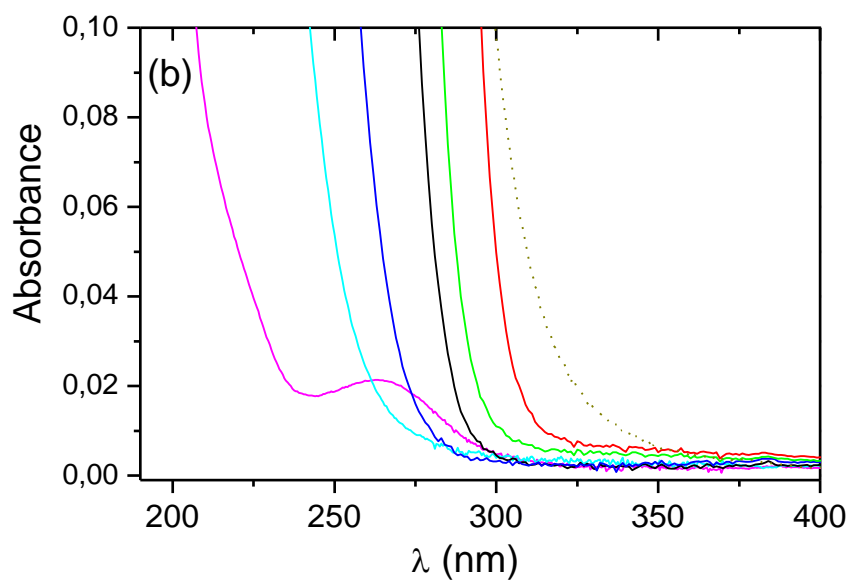
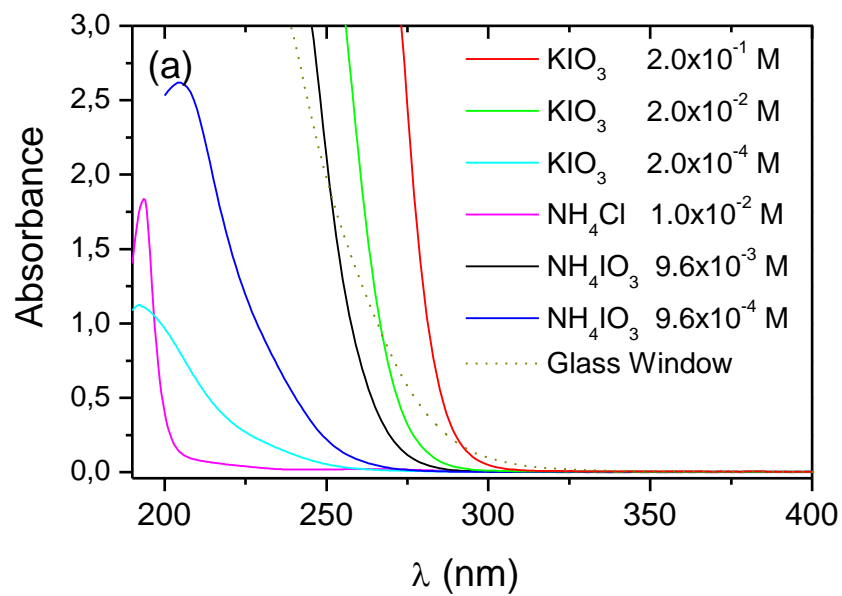
5



1

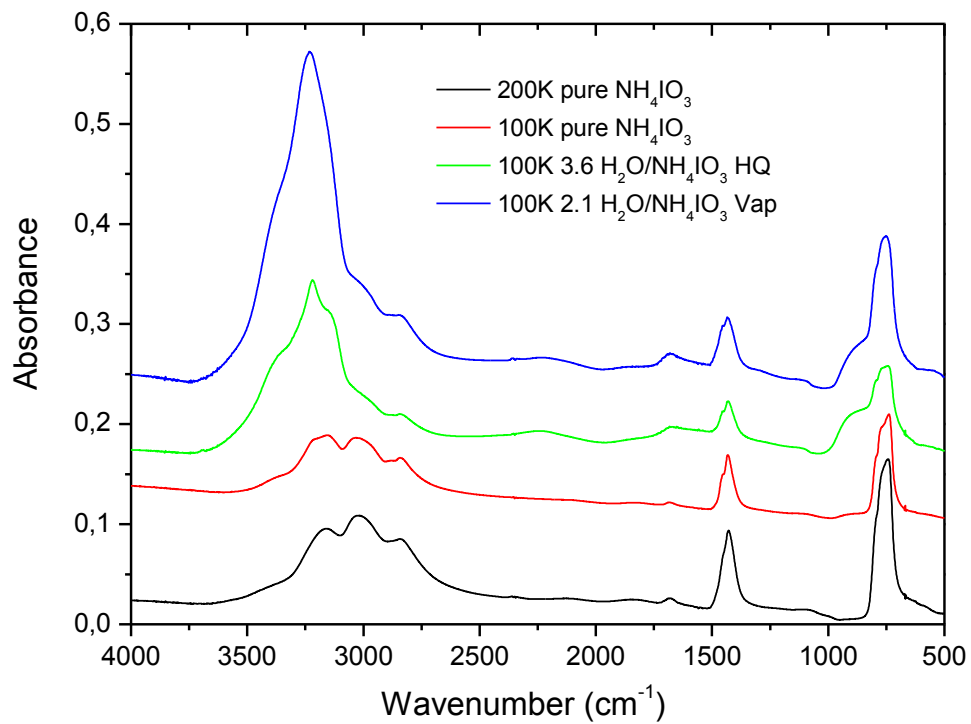
2 **Figure 1.** Schematic view of the experimental setup.

3



1
2
3
4
5
6

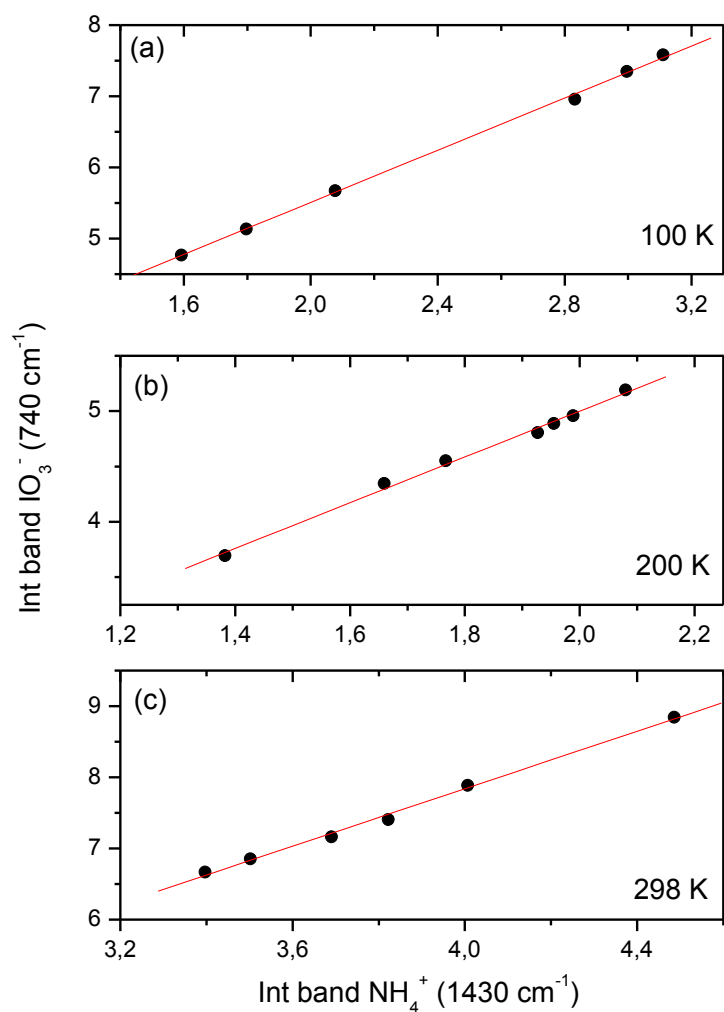
Figure 2. (a) UV-Vis absorption spectra from 190 to 400 nm for KIO_3 , NH_4Cl and NH_4IO_3 aqueous solutions. (b) Zoom-in of the low absorbance values.



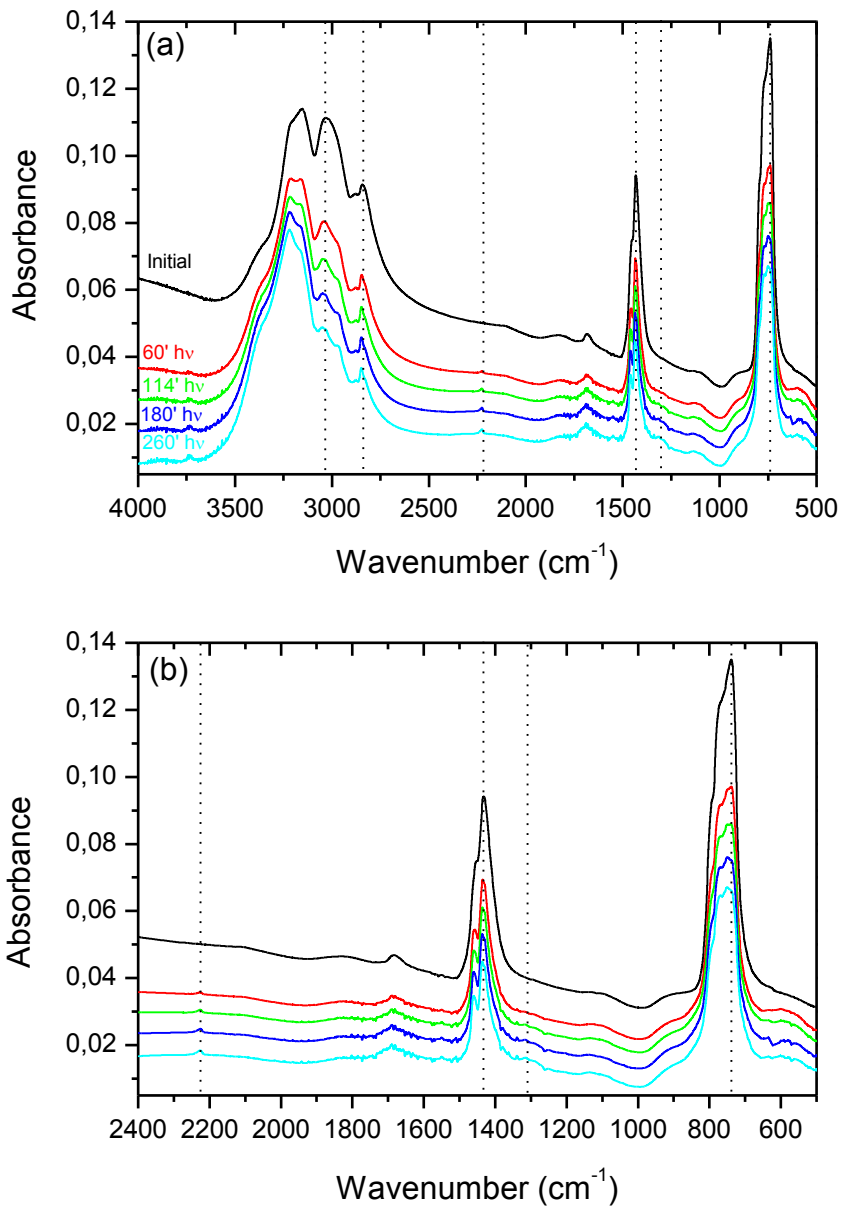
1
2

3 **Figure 3.** Mid-IR transmission spectra of pure NH₄IO₃ and H₂O/NH₄IO₃ ice mixtures
4 generated at different temperatures.

5



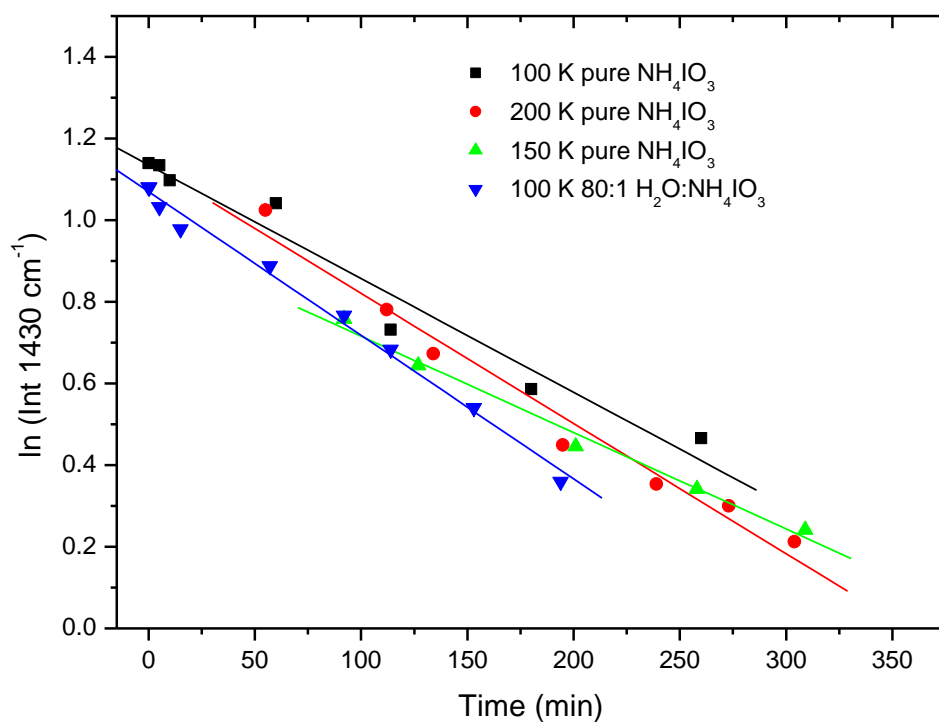
1
 2 **Figure 4.** Integrated intensities (in arbitrary units) of the v_4 band of NH_4^+ and the v_3 of IO_3^- of
 3 pure ammonium iodate samples generated and irradiated at (a) 100 K (b) 200 K and (c) 298
 4 K. Fit linear regression lines are shown in red.
 5



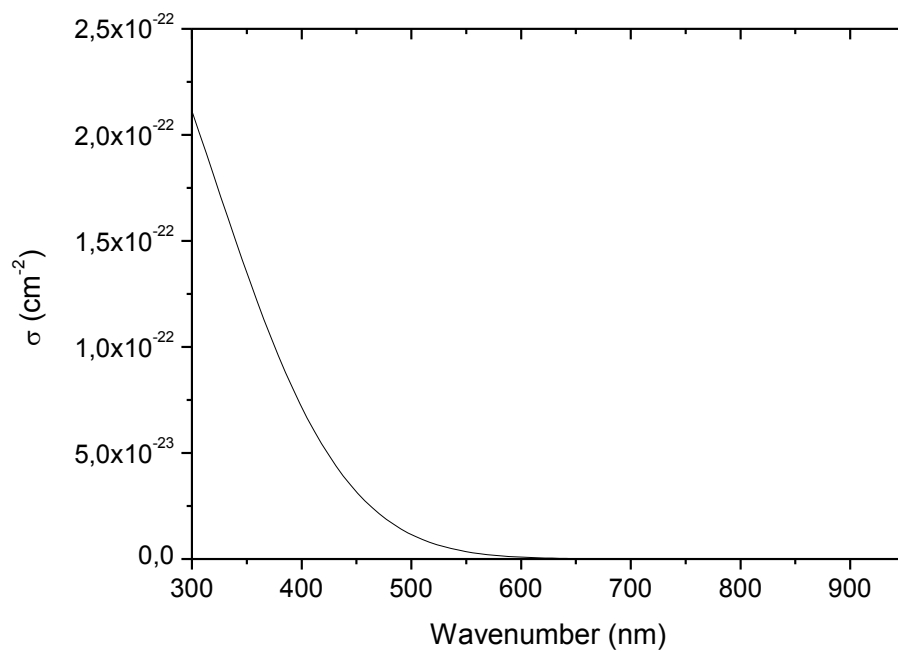
1

2 **Figure 5.** Evolution of the mid-IR transmission spectra of a pure NH_4IO_3 deposited at 100 K
 3 during photolysis at that temperature: Zero time, 60, 114, 180 and 260 min of photolysis in
 4 black, red, green, dark and light blue, respectively. The upper panel shows the whole IR
 5 spectra between 4000 and 500 cm^{-1} , the bottom panel is a zoom in the range 2400-600 cm^{-1} .
 6 Dotted lines indicate bands that undergo clear changes during the photolysis.

7



1
2 **Figure 6.** Representation of the natural logarithm of the integrated band intensity of NH_4^+ at
3 1430 cm^{-1} band versus photolysis time for some selected samples generated and irradiated at
4 different temperatures.
5
6



1

2 **Figure 7.** Simulated absorption cross section of iodate ion in a frozen ammonium iodate salt.

3